Journal of Hazardous Materials 175 (2010) 393–398

Contents lists available at ScienceDirect

Journal of Hazardous Materials

journal homepage: www.elsevier.com/locate/jhazmat

Uranium removal from groundwater by natural clinoptilolite zeolite: Effects of pH and initial feed concentration

Lucy Mar Camacho [a], Shuguang Deng [a,*], Ramona R. Parra [b]

[a] Department of Chemical Engineering, New Mexico State University, P.O. Box 30001, MSC 3805, Las Cruces, NM 88003, USA
[b] Physical Science Laboratory, New Mexico State University, P.O. Box 30001, MSC 3805, Las Cruces, NM 88003, USA

ARTICLE INFO

Article history:
Received 5 May 2009
Received in revised form 6 October 2009
Accepted 6 October 2009
Available online 13 October 2009

Keywords:
Uranium
Clinoptilolite
Adsorption
Equilibrium
Amphoteric

ABSTRACT

Adsorption of uranium (VI) on a natural clinoptilolite zeolite from Sweetwater County, Wyoming was investigated. Batch experiments were conducted to study the effects of pH and initial feed concentrations on uranium removal efficiency. It was found that the clinoptilolite can neutralize both acidic and low basic water solutions through its alkalinity and ion-exchange reactions with U within the solution, and adsorption of uranium (VI) species on clinoptilolite not only depends on the pH but also the initial feed concentration. The highest uranium removal efficiency (95.6%) was obtained at initial uranium concentration of 5 mg/L and pH 6.0. The Langmuir adsorption isotherm model correlates well with the uranium adsorption equilibrium data for the concentration range of 0.1–500 mg/L. From the experimental data obtained in this work, it was found that the zeolite sample investigated in this work is a mixture of clinoptilolite-Na zeolite and mineral impurities with a relatively large specific surface area (BET of 18 m^2/g) and promising adsorption properties for uranium removal from contaminated water.

1. Introduction

Uranium is present in the environment as a result of leaching from natural deposits, discharge from mill tailings, emissions from the nuclear industry, combustion of coal and other fossil fuels, and use of uranium-containing phosphate fertilizers. Naturally occurring uranium is a mixture of three radioisotopes (234U, 235U and 238U), but majority of them are 238U isotope (99.27%). Uranium is a radioactive heavy metal that can cause cancer. Its primary toxic effect when consumed in water is that of heavy metals [1,2]. Heavy metals, like uranium, lead, cadmium, and arsenic, are deposited in the kidneys and cause irreparable damage to the main filtering mechanism of the body. The maximum uranium level in drinking water recommended by the World Health Organization [3] is 15 μg/L, and the maximum contaminant level (MCL) set by the USEPA [4] for drinking water standard is 20 μg/L.

Several methods are available for removing uranium from drinking water. Ion-exchange is the most efficient removal method because it can remove about 98% of the uranium from water. However, it generates concentrated liquid wastes that must be disposed of. Other methods for removing uranium include chemical clarification that uses ferric sulfate or aluminum sulfate [5], precipitation [6], membrane filtration [7], and reverse osmosis [8]. The major limitation for these methods is the proper disposal of the resulting sludge that contains high levels of the metal and other contaminants.

Natural zeolites, a group of crystalline alumina-silicates with adsorption and ion-exchange capabilities, have gained increasing attention in drinking water purification [9,10,11]. Studies have been conducted to investigate the effects of sorption kinetics, pH, concentration, and temperature on uranium removal efficiency [12,13,14]. However, the initial concentrations reported in these studies covered a very limited range and no definite conclusion was drawn regarding its effect on uranium removal efficiency in the adsorption process.

The objective of this study was to investigate the effect of pH and initial concentration on the adsorption of uranium by a natural clinoptilolite zeolite from Sweetwater County, Wyoming. Batch adsorption equilibrium studies were carried out with aqueous solutions having initial uranium concentrations ranging from 0.01 mg/L to 500 mg/L. The experimental results obtained in this work will help us to understand the adsorption equilibrium and kinetics of uranium adsorption on natural clinoptilolite zeolite, and provide valuable insights on adsorption breakthrough process development and implementation.

2. Materials and methods

2.1. Characterization of adsorbent material

The natural clinoptilolite zeolite used in this study came from a zeolite deposit located Southeast of Bitter Creek in Sweetwater

* Corresponding author. Tel.: +1 575 646 4346 fax: +1 575 646 7706.
E-mail address: sdeng@nmsu.edu (S. Deng).

0304-3894/$ – see front matter © 2009 Elsevier B.V. All rights reserved.
doi:10.1016/j.jhazmat.2009.10.017

County, Wyoming. It was supplied by Gas Separation Technology, LLC, Denver, Co., USA. Physical and chemical properties of the clinoptilolite zeolite were determined by SEM, XRF, XRD, and N_2-adsorption analyses. Prior to SEM analysis the sample was sieved (mesh size 14 × 30), washed with distilled water, and dried at room temperature for 48 h. The dried zeolite sample was then coated with a gold film to alleviate charging and improve resolution, and placed in a scanning electron microscope (Hitachi S-3400N) for analysis.

Sample for crystal phase structure and crystal size analysis was crushed in a mortar and sieved (<325 mesh). Analysis was performed in a desktop Rigaku XRD apparatus (MiniFlex-II). The XRD pattern was obtained on a powder clinoptilolite zeolite sample (mesh <350) with a CuKa X-ray tube operated at 30 kV and 15 mA. By matching the XRD pattern with the built-in ICDD database in the equipment, we determined the crystal phase structure for the natural clinoptilolite zeolite.

Elemental analysis for major and trace elements in the clinoptilolite was made by using a Rigaku X-ray fluorescence analyzer (XRF) (ZSX, 100-e). Sample for major elemental analysis was prepared by mixing calcined natural clinoptilolite zeolite powder (325 mesh, 900 °C) with lithium tetraborate and lithium metaborate, and by placing the mixture in a muffle furnace at 1100 °C for 30 min. Sample for trace elemental analysis was prepared by mixing zeolite powder (325 mesh) with a binder solution (Ultra bind) in a steel pellet and by pressing the mixture at 20 ton in a press plate for 1 min. The dried samples were then placed in the XRF apparatus.

The BET and Langmuir specific surface area, pore size distribution, and pore volume of the natural clinoptilolite zeolite were determined in an accelerated surface area and porosimetry instrument (Micromeritics ASAP 2020). All the calculations were performed with the built-in software of the ASAP 2020 instrument. The Barrett–Joyner–Halenda (BJH) [15] and Horvath–Kawazoe (H–K) [16] models were selected for the calculation of the volume and pore size distribution.

2.2. Variation of pH with adsorption time

A 500 mg/L uranium stock solution was prepared from a calibration standard solution for ICP-MS containing 1000 mg/L of uranium (VI) oxide in 4% nitric acid. The calibration standard solution was provided by SPC Science, USA. Two 100 mL uranium solutions with 50 mg/L of concentration were prepared from the stock solution and adjusted with 0.10 M NaOH or 0.1 M HCl solution to pH 6.0 and 7.0 respectively. The solutions were then mixed with 1 g of clinoptilolite zeolite in 200 mL high density polyethylene plastic bottles. The bottles were tightly closed and placed in an automatic shaker (model lab-line Orbit No. 359) at 100 rpm for 100 h. A standard pH meter (Accumet Excel XL25, Fisher Scientific) was used during the batch adsorption experiments to monitor the changes on pH in the solutions, every half an hour during the first eight hours and then with decreasing frequency.

2.3. Effect of pH on uranium adsorption

The effect of pH on the uranium adsorption equilibrium was investigated at acidic and basic conditions. The initial pH of 100 mL uranium solutions with 10 mg/L of concentration was adjusted to 3.0, 5.0, 6.0, 7.0, and 9.0 by adding 0.1 M HCl or 0.1 M NaOH solution. The solutions were then mixed with 1 g of clinoptilolite zeolite in 200 mL plastic bottles, closed tightly, and placed in the automatic shaker at 100 rpm. The experiment was conducted under batch conditions for five days to ensure that adsorption equilibrium was obtained. Initial and final pH values were recorded. After stabilization, samples were removed, filtered (0.45 μm nylon) and analyzed with an ICP-MS Spectrometer (Elan DRC-e, Perkin Elmer).

Table 1
Elemental analysis for the natural clionoptilolite zeolite.

Major elements	Concentration wt (%)	Trace elements	Concentration (mg/g)
SiO_2	64.9	Rb	84
TiO_2	0.2	Th	19.8
Al_2O_3	12.9	Nb	25
Fe_2O_3	1.4	Sr	415
MnO	0.01	Zr	262
MgO	0.7	Y	24.9
CaO	1.7	Pb	23.1
Na_2O	4.4	U	4.2
K_2O	1.6	Cr	23
P_2O_5	0.04	Ni	11
Loss on ignition	11.5	Cu	96
		Zn	71
		Ga	16.4

2.4. Equilibrium adsorption of uranium on clinoptilolite zeolites

Uranium solutions with initial concentration ranging from 0.01 mg/L to 500 mg/L were prepared by diluting the corresponding volume of the standard stock solution of 500 mg/L with deionized water (Milli-Q System, resistivity of 18.2 MΩ cm, TOC ≤10 μg/L) to complete 195 mL in 200 mL plastic bottles. The pH of the solutions was adjusted to 6.0 to mimic the drinking water purification condition by adding 0.10 M NaOH or 0.1 M HCl solution. The pH of all solutions was measured with the standard pH meter, and the uranium concentration in the water samples was analyzed with ICP-MS. Two grams of the natural clinoptilolite zeolite sample were added to each bottle. The bottles were then closed tightly and placed in the automatic shaker that was set at a shaking speed of 100 rpm. Based on observed pH variations in the solutions in contact with clinoptilolite after 100 h, the batch adsorption experiments conducted in this work were run continuously for five days to ensure the adsorption equilibrium point for each concentration analyzed. The water samples were then removed from the shaker, filtered (0.45 μm nylon), and analyzed with ICP-MS for uranium concentration. A simple mass balance on the water solution and the adsorbent was carried out to calculate the adsorption amount on the natural clinoptilolite zeolite for each solution concentration. The final uranium concentration remaining in solution was defined as the equilibrium concentration. The adsorption capacity (mg/g) in equilibrium with the final concentration was obtained by dividing the adsorbed amount (mg) with the mass of the adsorbent (2 g).

3. Results and discussion

3.1. Characterization of clinoptilolite

The major and trace elements of the natural clinoptilolite zeolite investigated in this work were determined by XRF elemental analysis and summarized in Table 1. Except for the major components Si and Al, Na is the next component with 4.4 wt.%. The silica to alumina ratio (Si/Al = 5.0) for the clinoptilolite studied provides relatively high negative charges for attracting positive uranium (VI) species. The Si/Al ratio is the most important parameter that determines the crystal structure and ionic charges of the clinoptilolite zeolite as an adsorbent material.

The XRD data of the clinoptilolite zeolite were processed with the Jade 8 XRD analysis software. The data matches well with that of Na-Clinoptilolite (sodium form of clinoptilolite), which has the empirical chemical formula $(Na, K, Ca)_2\text{-}3(Si,Al)_{18}O_{36}{\cdot}11H_2O$ [17]. This finding is consistent with the XRF elemental analysis results listed in Table 1. Some small amorphous particles surrounding the clinoptilolite crystal clusters can be seen in the SEM image of the natural clinoptilolite zeolite shown in Fig. 1. The presence of quartz

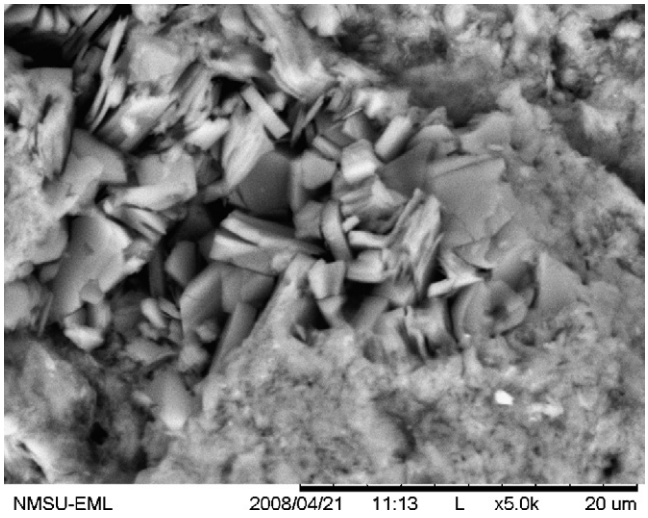

Fig. 1. SEM Image of the natural clinoptilolite zeolite (Magnification = 5.0 K, Scale Bar = 20 μm).

on clinoptilolite zeolite samples from the same deposit is being reported by Hulbert [18]. He also reported that no other mineral phases were recognized by XRD. These amorphous particles may have different pore structures and adsorption properties than the natural clinoptilolite zeolite.

Fig. 2(A) shows the N_2-adsorption and desorption isotherms obtained at the liquid nitrogen temperature (−196 °C) with the ASAP analyzer. A small desorption hysteresis loop was observed, suggesting that a pure condensation occurred with no adsorption into layers [19]. According to the lattice theory concepts used by Donohue and Aranovich [20], the formation of the hysteresis is caused by the presence of finite-length pores due to the differences that exist in the interface shape of these pores. The slope of the hysteresis is characteristic of the presence of mesopores in the material.

The specific surface area, the microporous volume and the pore properties were calculated with the built-in software of the ASAP equipment. Table 2 summarizes the pore textural properties for the studied clinoptilolite. The observed BET surface area for the clinoptilolite zeolite is 18 m^2/g, which is similar to a reported BET surface area of 16.8 m^2/g for zeolitic volcanic tuff [21]. It is also higher than the BET surface area of coconut shell carbon (2.82 m^2/g) [22]. The Langmuir surface area is 165 m^2/g. The main difference between the observed BET and Langmuir surface areas is given by the fact that the adsorption in the micropores/mesopores is not governed by the BET equation, because multilayer adsorption in the micropores is impossible [23].

Fig. 2(B) shows the pore size distribution for the clinoptilolite zeolite obtained from the desorption isotherm following the BJH and H–K models [15,16]. The BJH model was developed to determine volume and pore size distributions between l7 Å and 3000 Å. It accounts for both the change in adsorbed layer thickness and the liquid condensed in the pore volume.

The H–K model determines the volume and pore size distributions for smaller pore sizes. The BJH described well the pore size distribution within the studied clinoptilolite zeolite. The first peak in the graph represents the micropore distribution, and the second peak the macropores/mesopores distribution. The clinoptilolite zeolite has an average pore size of 166 Å. It also has a pore volume of 0.027 cm^3/g. This last value is consistent with the reported pore volume of 0.037 cm^3/g for a natural Na-modified clinoptilolite [24].

Table 2
Summary of pore textural properties for the natural clinoptilolite zeolite.

BET surface area (m^2/g)	18
Langmuir surface area (m^2/g)	118
BJH pore volume (cm^3/g)	0.065
H–K maximum pore volume (cm^3/g)	0.027
BJH average pore size (Å)	166
H–K median pore size (Å)	95

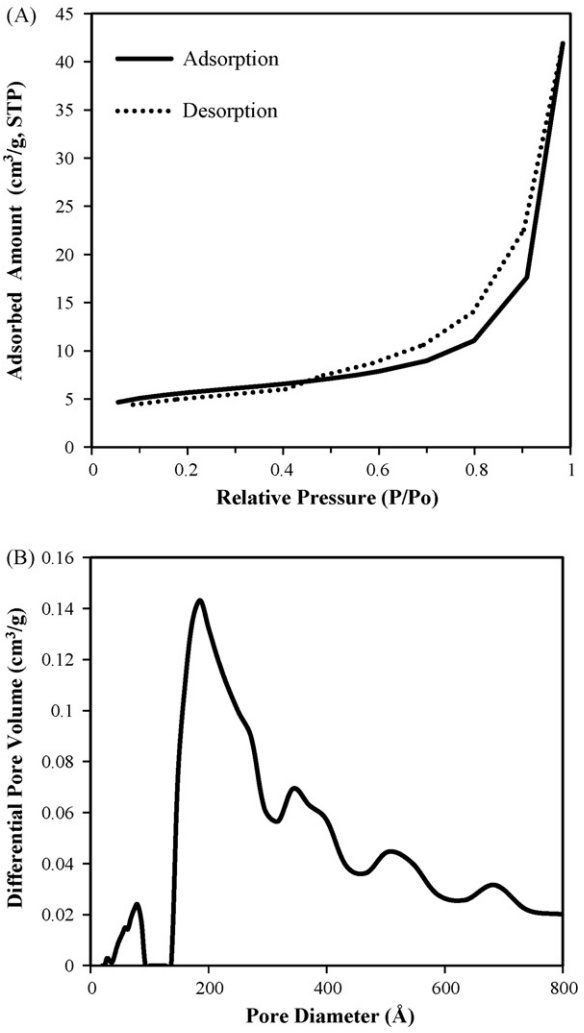

Fig. 2. (A) N_2-adsorption and desorption isotherms for the natural clinoptilolite zeolite at 77 K; (B) Pore size distribution for the natural clinoptilolite zeolite.

3.2. Variation of pH with adsorption time

Analysis of pH changes with adsorption time was conducted to observe the pH variation during adsorption and to determine the minimum time required for obtaining adsorption equilibrium. Fig. 3 displays the experimental data for two solutions with initial pH values of 6.0 and 7.0. The overall trends of pH variation with time for these two sets of experiments at pH of 6.0 and 7.0 are almost the same except for the initial 2 h. For the solution with an initial pH of 6.0, the pH increased of the solution increased steadily from 6.0 to 6.8 during the first 2 h, decreased from 6.8 to 6.5 in the next 3 h, then increased again and keep increasing slowly. A slightly different trend was observed for the solution with an initial pH of 7.0. The pH of this solution decreased from 7.0 to 6.5 during the first 15 min, it then followed a similar route of pH change with time as observed in the solution with an initial pH of 6.0. The variation of pH during the first 5 h of the adsorption process may be the result of neutralization

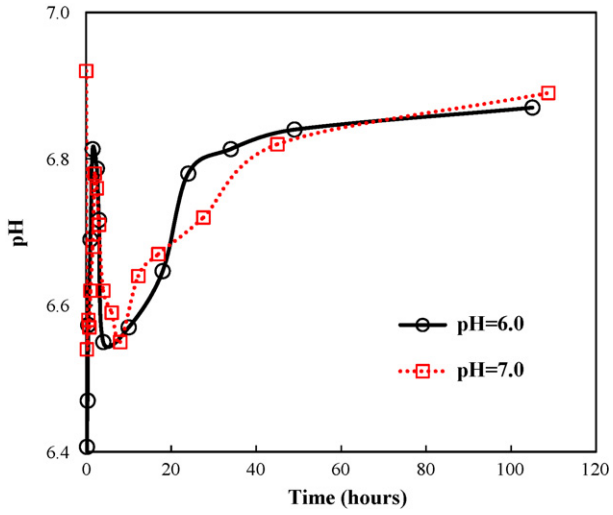

Fig. 3. Variation of solution pH with adsorption time on natural clinoptilolite zeolite at 25 °C and initial concentration of 50 mg/L.

reactions as well as adsorption or ion-exchange reactions of the uranium with the zeolite. Filippidis and Kantiranis [25] observed similar phenomena by adding Ca-rich clinoptilolite zeolite into an acidic water stream and a basic lake water and attributed these behaviours to the amphoteric properties of the zeolite. After the initial 5 h, the pH of the two solutions increased steadily meaning that more uranium ions are removed by physical adsorption and ion-exchange. After 100 h, the pH for both samples appears to still be increasing. Based on above observations we can conclude that the clinoptilolite zeolite can neutralize both weak acid and weak basic solutions through its alkalinity and ion-exchange reactions within the solution.

3.3. *Effect of pH on uranium adsorption*

The adsorption equilibrium of uranium as a function of pH was studied to determine the optimum pH at which highest metal adsorption occurs. An initial concentration of 10 mg/L was used for all the experimental runs. The pH of the solution was closed monitored with the change in uranium concentration. The experimental data of initial and final uranium concentration versus pH are presented in Fig. 4(A). The variation of the uranium adsorption amount with initial pH is illustrated in Fig. 4(B). In all cases covering pH from 3 to 9, the equilibrium concentrations were lower than the initial solution concentrations, suggesting that removal of uranium by the zeolite occurred. The minimum uranium adsorption occurred at pH 9.0. A maximum U adsorption capacity of 0.7 mg/g was obtained at pH 6.0. The observed pH behaviour can be explained by the presence of different mononuclear and polynuclear uranium (VI) hydrolysis products in the form $[(UO_2)_p(OH)_q]^{(2p-q)+}$ at different pH values and metal concentrations in the solution [26]. The uranyl ion (UO_2^{2+}) (Eq. (1)) is the dominant species at pH lower than 3.0. At pH of 3.0 the mononuclear hydrolysis product of the uranyl ion, $UO_2(OH)^+$ (Eq. (2)), is readily formed and available to be adsorbed. At pH between 3.0 and 5.0 the polynuclear products $(UO_2)_2(OH)_2^{2+}$ (Eq. (3)), $(UO_2)_3(OH)_4^{2+}$ (Eq. (4)), and $(UO_2)_3(OH)_5^+$ (Eq. (5)) are also present and available for adsorption. At pH higher than 5 the hydrolysis is more intense and an additional polynuclear product, $(UO_2)_4(OH)_7^+$ (Eq. (6)), is formed [27]. These species can be readily adsorbed or ion-exchanged by the clinoptilolite.

$$UO_2(OH)_2 \leftrightarrow UO_2^{2+} + 2OH^- \quad (1)$$

$$UO_2^{2+} + H_2O \leftrightarrow UO_2(OH)^+ + H^+ \quad (2)$$

$$2UO_2^{2+} + 2H_2O \leftrightarrow (UO_2)_2(OH)_2^{2+} + 2H^+ \quad (3)$$

$$3UO_2^{2+} + 4H_2O \leftrightarrow (UO_2)_3(OH)_4^{2+} + 4H^+ \quad (4)$$

$$3UO_2^{2+} + 5H_2O \leftrightarrow (UO_2)_3(OH)_5^+ + 5H^+ \quad (5)$$

$$4UO_2^{2+} + 7H_2O \leftrightarrow (UO_2)_4(OH)_7^+ + 7H^+ \quad (6)$$

This explains the observed increase of uranium adsorbed at pH below 6.0. However, at pH of 6.0, a stable precipitation product, $UO_2(OH)_2$, can be formed and therefore the adsorption has to compete with the precipitation reactions. At pH higher than 6.0 the polynuclear species $(UO_2)(OH)^+$, $(UO_2)_2(OH)_2^{2+}$, and $(UO_2)_3(OH)_4^{2+}$, are not available anymore and the presence of species $(UO_2)_3(OH)_5^+$ is also limited until it finally disappear with increasing pH (Fig. 4) [6,27]. Adsorption of uranium is limited at pH above 9.0 because no sufficient hydrolysis products are available at such a high pH, which explains well the minimum adsorption of uranium at pH of 9.0 in Fig. 5. The presence of competing carbonate complexes of U(VI) is not taken into account, because the selected experimental conditions involved the presence of CO_2 pressures less than atmospheric CO_2 (solution containers were tightly closed) [28]. Based on the observed pH behaviour, a pH of 6.0 was chosen for batch adsorption experiments with different initial concentrations to measure the adsorption isotherm.

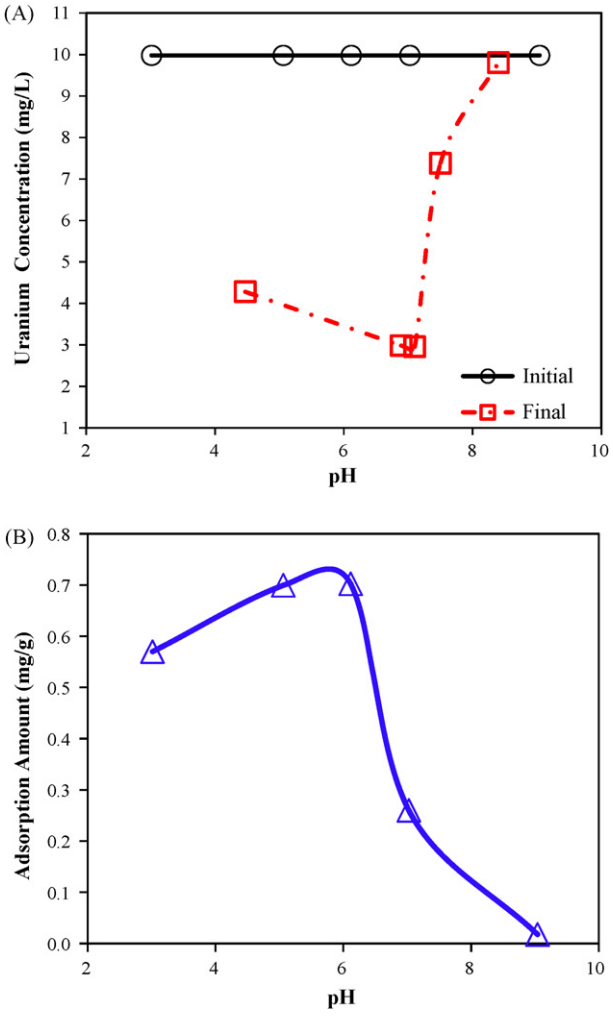

Fig. 4. (A) Effect of solution pH on uranium adsorption equilibrium concentration at pH 6.0 and 20 °C; (B) Uranium adsorption amount at pH 6.0 and 25 °C.

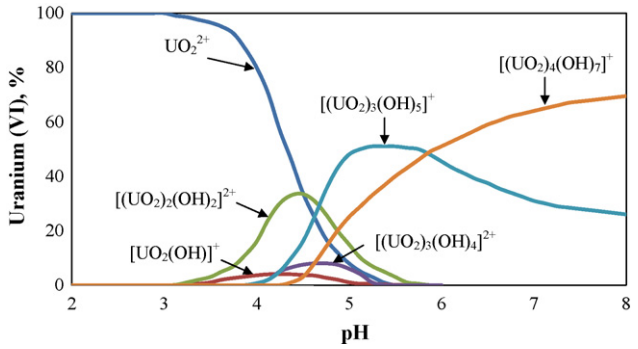

Fig. 5. Percentage distribution of uranium (VI) species for a total concentration of 10^{-3} M (adapted from Misaelides et al. [27].

3.4. Effect of initial concentration on uranium removal efficiency

The effect of initial concentration on the adsorption of uranium (VI) by clinoptilolite at pH 6.0 was analyzed by calculating the distribution coefficient and the percentage of uranium removal from the experimental equilibrium data obtained at different initial concentrations. The clinoptilolite uptake distribution coefficient can be calculated from the following equation [13]

$$K_d = \frac{q_e}{C_e} \quad (1a)$$

where K_d is the adsorption uptake in (L/g) and it represents the ratio of the uranium concentration in the solid (mg/g) and liquid phase (mg/L).

Fig. 6 displays variation of uranium removal efficiency and uranium adsorption distribution coefficient as a function of initial uranium solution concentration. Both adsorption distribution coefficient and uranium removal efficiency increased with the increase of initial uranium concentration and reached their maxima at the initial concentration of 5 mg/L. The maximum uranium adsorption distribution coefficient and maximum removal efficiency shown in Fig. 6 are 2.12 mg/L and 95.6%, respectively. The sharp decrease of K_d with the initial solution concentration after the maximum suggests a rapid saturation of active sites available for uranium adsorption, and the presence of competing reactions, specifically the uranium precipitation reactions, that may significantly reduce

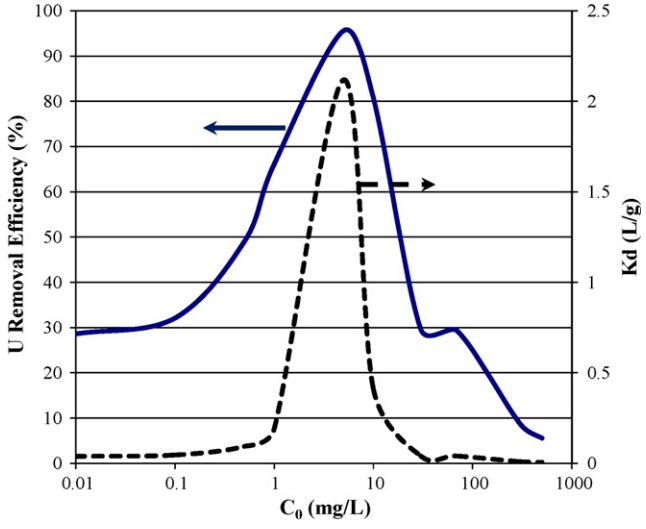

Fig. 6. Removal efficiency and adsorption distribution coefficient of uranium on the natural clinoptilolite zeolite at pH of 6.0 and 25 °C.

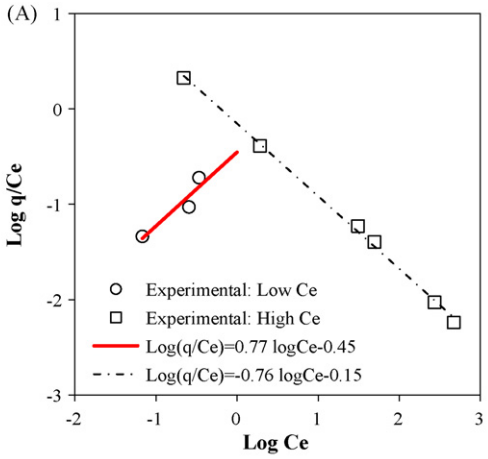

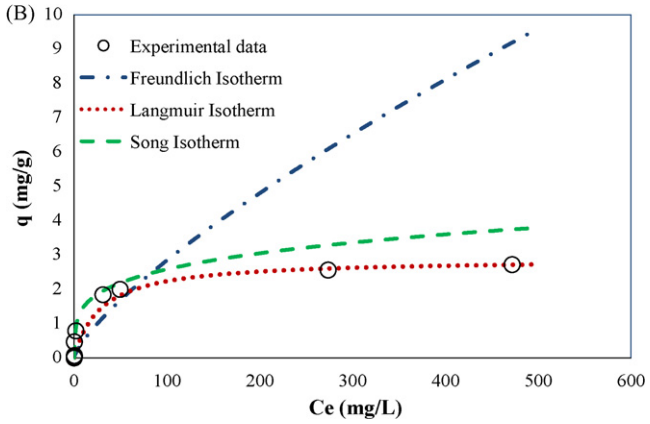

Fig. 7. (A) Linear plots of Song's isotherm at low and high concetration ranges; (B) comparison of model correlations of experimental isotherm data for uranium adsorption on natural clinoptilolite at pH of 6.0 and 25 °C.

the uranium ions available for adsorption. Yellow uranium precipitates were observed in the batch adsorption experiments with solution concentrations of 30–500 mg/L. The intensity of the yellow color and the amount of precipitates increased with increasing solution concentration. The maximum in Fig. 6 can be attributed to the presence of the polynuclear species $(UO_2)_4(OH)_7^+$. This species is present in small quantities in the speciation diagram for uranium at pH 6.0 and concentration of 1 mg/L [26,6] but is the major ionic species present in the speciation diagram for uranium at the same pH but at a concentration of 230 mg/L [26,27]. Aytas et al. [13] reported a maximum uranium adsorption distribution coefficient and removal efficiency of 351 L/g and 88% respectively at pH 2.0 and initial concentration of 25 mg/L. The high distribution coefficient and removal efficiency reported by Aytas et al. [13] can be attributed to the presence of the uranyl ion (UO_2^{2+}) which is the dominant hydrolysis species for any U solubility concentration at this low pH. Purification of drinking water under pH 2.0 is not feasible because this pH does not mimic drinking water purification conditions.

3.5. Adsorption isotherms

The uranium adsorption equilibrium data obtained at pH of 6.0 and initial solution concentrations from 0.01 mg/L to 500 mg/L are plotted in Fig. 7(A). In addition to the traditional Freundlich and Langmuir adsorption isotherm models, the Song isotherm model was used to correlate the experimental data.

Table 3
Summary of adsorption isotherm model parameters.

Freundlich	Langmuir	Song
K = 0.08754 L/g $1/n$ = 0.7558	a = 2.8793 mg/g b = 0.0347 L/mg	K = 0.6357 L/g β = 0.4533 (mg/L)$^{-2}$ n = 0.239
R^2 = 0.7895	R^2 = 0.9795	R^2 (Low Ce) = 0.958 R^2(High Ce) = 0.997

The Freundlich isotherm model [29] indicates the heterogeneity of the adsorbent material and is given by the equation

$$q = K C_e^{1/n} \tag{2a}$$

where q (mg/g) is the amount of uranium adsorbed at equilibrium, C_e (mg/L) is the equilibrium concentration, K (L/g) and n are the Freundlich constants related to the zeolite adsorption capacity and adsorption intensity, respectively.

The Langmuir isotherm model [30] assumes the formation of a monolayer onto the adsorbent surface with a finite number of identical sites, and is given by the equation

$$q = \frac{a\,b\,C_e}{1 + K\,C_e} \tag{3a}$$

where C_e (mg/L) is the uranium equilibrium concentration, and a (mg/g) and b (L/mg) are the Langmuir constants related to the capacity and energy of the adsorption, respectively.

The Song isotherm model [31] was developed to describe adsorption data covering a wide range of concentrations. It assumes that the Henry's law and the Freundlich isotherm model are satisfied in the low and high concentration ranges, respectively. The equation representing the model is given by

$$q = K(1 + \beta C_e{}^2)^{(n-1)/2} C_e \tag{4a}$$

where K (L/g) is the partition coefficient in the Henry's law region and is estimated from the ordinate value of the asymptote in the low concentration region. The Freundlich index n is obtained from the slope of the asymptote in the high concentration region. The parameter β (mg/L)$^{-2}$ corresponds to the intersection point between the two concentration regions, and is estimated from the intersection point of the two asymptotes.

Fig. 7(A) shows the linear plots of the Song model for the low (0.01–10 mg/L) and high (10–500 mg/L) concentration ranges. The R^2 values for the low and high concentrations are 0.958 and 0.997, respectively. The values for the parameters K, β, and n in the Song model are presented in Table 3. The parameters for the Freundlich and Langmuir models are also included in the Table 3. Comparison of the correlations by the models is shown in Fig. 7(B). The Freundlich isotherm model can't correlate the experimental data well. Although the Song isotherm model is supposed to address the issues of adsorption in a wide range of solution concentration, it failed to describe the experimental data of uranium adsorption on the natural clinoptilolite zeolite. As reported by Ayoob [32] it is very challenging to correlate adsorption isotherm at high adsorbate concentrate range. The Langmuir isotherm fits the entire data well and gives the best correlation among the three models tested in this work (R^2 = 0.9797).

4. Conclusions

A natural clinoptilolite zeolite from Sweetwater County, Wyoming was characterized and evaluated for uranium adsorption to explore the feasibility of using this inexpensive adsorbent for uranium removal from drinking water. It was found that the natural clinoptilolite zeolite sample investigated in this work is a mixture of clinoptilolite-Na zeolite and mineral impurities with a reasonably large specific surface area (BET of 18 m^2/g). The silica to alumina ratio for the studied clinoptilolite (Si/Al = 5.0) suggests that it has relatively high negative charges to bind the positive uranium (VI) ions from water. Adsorption experiments performed in this work have proven that this natural clinoptilolite zeolite can effectively absorb uranium from water at different pH and initial uranium concentrations. The zeolite adsorbent has the highest uranium (VI) adsorption distribution coefficient of 2.12 mL/g and the maximum uranium removal efficiency of 95.6% at initial uranium concentrations of 5 mg/L and pH of 6.0. The uranium adsorption strongly depends on the pH and the initial concentration due to the amphoteric properties of the radioisotope. These two parameters determine the amount and type of hydrolysis products readily available for adsorption. Three adsorption isotherm models were applied to correlate the uranium adsorption equilibrium data. The Langmuir isotherm model gives the best correlation among all three models tested in this work.

Acknowledgment

The authors would like to thank Dr. Nancy McMillan of Geological Sciences Department at New Mexico State University for her assistance with the XRF measurements, and Dipendu Saha for his support with the N_2-adsorption measurements. The financial support of this work provided by the office of the Vice President for Research at New Mexico State University is gratefully acknowledged.

References

[1] World Health Organization (WHO), Uranium in Drinking water: Background document for development of WHO guidelines for drinking water quality (WHO/SDE/WSH/03.04/118), World Health Organization, 2005, 26 pp.
[2] A.C. Hakonson-Hayes, P.R. Fresquez, F.W. Whicker, J. Environ. Radioact. 59 (1) (2002) 29–40.
[3] World Health Organization, Guidelines for Drinking Water Quality, Third Edition, Incorporating the First and Second Addenda, Volume 1, Recommendations, Geneva, 2008, 515 pp.
[4] EPA, Radionuclides Notice of Data Availability, Technical Support Document, USEPA Office of Groundwater and Drinking Water, March 2000, 164 pp.
[5] A. Baeza, M. Fernandez, M. Herranz, F. Legarda, C. Miro, A. Salas, Water, Air, Soil Pollut. 173 (2006) 57–69.
[6] A. Krestou, A. Xenidis, D. Panias, Miner. Eng. 17 (3) (2004) 373–381.
[7] S. Chellam, D.A. Clifford, J. Environ. Eng. 128 (10) (2002) 942–952.
[8] K.L. Lin, M.L. Chu, M.C. Shieh, Desalination 61 (2) (1987) 125–136.
[9] A. Krestou, A. Xenidis, D. Panias, Miner. Eng. 16 (12) (2003) 1363–1370.
[10] H. Faghihian, R.S. Bowman, Water Res. 39 (2005) 1099–1104.
[11] R.S. Bowman, Microporous Mesoporous Mater. 61 (2003) 43–56.
[12] R.G. Reddy, C. Zhengan, Light Met. (1996) 1173–1180.
[13] S.M. Aytas, S. Akyil, M. Eral, J. Radioanal. Nucl. Chem. 260 (1) (2004) 119–125.
[14] A. Kilincarslan, S. Akyil, J. Radioanal. Nucl. Chem. 264 (3) (2005) 541–548.
[15] E.P. Barrett, L.G. Joyner, P.P. Halenda, J. Am. Chem. Soc. 73 (1951) 373–380.
[16] G. Horvath, K. Kawazoe, J. Chem. Eng. Jpn. 16 (6) (1983) 470–475.
[17] J.R. Boles, Am. Mineral 57 (1972) 1363–1493.
[18] M.H. Hulbert, Clays Clay Miner. 35 (6) (1987) 458–462.
[19] D.D. Do, Adsorption Analysis: Equilibrium And Kinetics, Imperial College Press, Singapur, Singapore, 1998, pp 892.
[20] M.D. Donohue, G.L. Aranovich, J. Colloid Interface Sci. 205 (1) (1998) 121–130.
[21] D. Humelnicu, G. Drochioiu, M.I. Sturza, A. Cecal, K. Popa, J. Radioanal. Nucl. Chem. 270 (3) (2006) 637–640.
[22] R.S. Sathish, N.R. Raju, G.N. Rao, K.A. Kumar, C. Janardhana, Sep. Sci. Technol. 42 (2007) 769–788.
[23] M.J. Remy, G.A. Poncelet, J. Phys. Chem. 99 (2) (1995) 773–779.
[24] M.W. Ackley, R.T. Yang, Eng. Che. Res. 80 (1991) 2523–2530.
[25] A. Filippidis, N. Kantiranis, Desalination 213 (1–3) (2007) 47–55.
[26] C.F. Baes Jr., R.E. Mesmer, The Hydrolysis Of Cations, John Wiley & Sons, New York, 1976, pp 489.
[27] P. Misaelides, A. Godelitsas, A. Filippidis, D. Charistos, I. Anousis, Sci. Total Environ. 173 (1–6) (1995) 237–246.
[28] J. Prikril, A. Jain, D.R. Turner, R.T. Pabalan, J. Contam. Hydrol. 47 (2001) 241–253.
[29] H.M.F. Freundlich, Z. Phys. Chem. (1906) 385–470.
[30] I. Langmuir, J. Am. Chem. Soc. 40 (1916) 1361–1403.
[31] D.I. Song, W.S. Shin, Environ. Sci. Technol. 39 (2005) 1138–1143.
[32] S. Ayoob, A.K. Gupta, J. Hazard. Mater. 152 (2008) 976–985.